Finite Element Simulation of Nd:YAG laser lap welding of AISI 304 Stainless steel sheets

N. SIVA SHANMUGAM[1*], G. BUVANASHEKARAN[2] AND K. SANKARANARAYANASAMY[1]
[1]Department of Mechanical Engineering, National Institute of Technology, Tiruchirappalli – 620015, Tamil Nadu, India.
[2]Advanced Welding Group, Welding Research Institute, Bharat Heavy Electricals Limited, Tiruchirappalli – 620014, Tamil Nadu, India.
[*]nsiva@nitt.edu http://www.nitt.edu

Abstract: - Laser beam welding (LBW) is one of the most important manufacturing processes used for joining of materials. It is also a remarkably complicated, nonlinear operation involving extremely high temperatures. Since its invention more than two decades ago, laser beam welding has been more of an art than a science. Laser welding of austenitic stainless steel AISI 304 the candidate material of this research work is used in several areas, including electronics, medical instruments, home appliances, automotive and specialized tube industry. An industrial 2kW CW Nd:YAG laser system, available at Welding Research Institute (WRI), BHEL Tiruchirappalli, is used for conducting the welding trials for this research. After proper tuning of laser beam, laser welding experiments are conducted on AISI 304 grade sheets for lap joint configuration to evaluate the influence of input parameters such as beam power, welding speed and spot diameter of the beam on weld bead geometry i.e. bead width (BW) and depth of penetration (DOP). Three dimensional finite element simulation of high density heat source is performed for laser welding technique using finite element code SYSWELD for predicting the temperature profile on AISI 304 stainless steel sheets. The temperature dependent material properties for AISI 304 stainless steel are taken into account in the simulation, which has a great influence in computing the temperature profiles. The latent heat of fusion is considered by the thermal enthalpy of material for calculation of phase transition problem. A Gaussian distribution of heat flux using a moving heat source with a conical shape is used for analyzing the temperature profiles. Experimental and simulated values for weld bead profiles are analyzed for stainless steel material for different beam power, welding speed and beam spot diameter. The results obtained from the simulation are compared with those from the experimental data for laser welding of lap joint configuration and it is observed that the results of numerical analysis (FEM) are in good agreement with experimental results, with an overall percentage of error estimated to be within ±5%.

Key-Words: - Laser welding, Heat source, SS 304, lap joint, FEM, SYSWELD, Nd:YAG laser

1 Introduction

Laser keyhole welding is a complex process involving thermodynamic cycles, fluid flows and heat transfer phenomena among others. It is a high energy density welding process, which has the possibility of focusing the beam to a very small spot diameter. As a result, it has been increasingly utilized in all industrial sectors like automobile, ship building, electronic industry, etc. Laser welding offers significant advantages over other welding processes (Gas Tungsten Arc welding, Gas Metal Arc Welding, Friction Welding, Induction Welding, etc.) in terms of penetration depth, heat affected zone, heat input and thermal distortion. In laser welding, the pressure created by the intense vaporization tends to dig the molten metal zone, which allows the laser beam to penetrate deeper in the material, making the irradiated zone a thin hole, known as keyhole [1]. Moving the laser head and the associated keyhole will cause the flow of the molten metal surrounding the keyhole to the rear region where it solidifies to form a weld bead. The molten pool shape and weld quality of laser welds produced by using a Continuous Wave Nd:YAG laser welding machine depends on various process parameters. Generally, laser beam welding involves many variables: beam power, welding speed, spot diameter, beam incident angle, type of shielding gas and gas flow rate. When developing the welding procedure for a specific application, each of these process parameters must be optimized, characterized and fully specified. This is usually done by conducting welding experiments on trial and error basis, which leads to high operative difficulties and increasing total cost of the process. The current computing technology and finite element based numerical techniques have improved to the point where numerical modelling has begun to take shape as a realistic method for the prediction of temperature profiles and weld bead geometry.

A brief literature review on weld process analysis and weld pool modelling is outlined here. The elementary welding heat source models were based mostly on Rosenthal's solutions [2]. He proposed a mathematical model for a moving heat source under the assumptions of quasi-stationary state and concentrated point heating in 3D analysis. Sabbaghzadeh et al [3] developed two numerical models in finite difference and finite element, to compute thermal phenomena during pulsed laser welding. They found that the temperature contours and depth of penetration were strongly dependent on the pulse parameters of the laser beam. Spina et al [4] investigated the efficiency of numerical simulations to predict the thermo-mechanical fields induced by laser welding of aluminum alloy sheets. The penetration depth, nugget size and bead width of laser spot welds on AISI304 stainless steel were studied by Chang and Na [5] using the finite element method and artificial neural network. There are many research papers which deal with the shape and size of the molten pool of laser beam butt welds in relation to different laser input parameters. However, the effect of main laser parameters namely beam power, welding speed and beam spot diameter on lap joint welds have till date not been reported in detail. Since the sheets are placed one and another in lap joint configuration, the beam should penetrate the top sheet and get into the bottom sheet. Hence, the effect of beam spot diameter on weld bead geometry has to be analyzed in depth.

This paper presents the thermal field and the bead shape of a lap joint made of AISI304 stainless steel sheet by laser welding, using FE transient thermal analysis. The heat source model is assumed to be a 3D conical Gaussian and the required FORTRAN subroutines are developed in order to define a moving distributed heat source for the simulations carried out using finite element code SYSWELD. The depth of penetration and bead width of lap joint laser welds obtained by simulation methods are compared with the lap joints weld specimens produced using the same welding parameters for validation.

2 Heat Transfer Analysis

To identify the relationships between the molten pool shape and the laser welding parameters, it is necessary to first study the effects of the laser process parameters on the temperature field induced by laser irradiation. The coordinate system of laser welding used in this work is shown in Fig. 1. It is assumed that a laser beam with Conical Gaussian distribution [6] moves with a constant velocity v along the x-axis. In general, the governing equation of heat conduction for the three dimensional transient temperature can be written as [22]:

$$\rho(T)c(T)\frac{\delta T}{\delta t} + v\rho(T)c(T)\frac{\delta T}{\delta x} = \frac{\delta}{\delta x}\left(k_x\frac{\delta T}{\delta x}\right) + \frac{\delta}{\delta y}\left(k_y\frac{\delta T}{\delta y}\right) + \frac{\delta}{\delta z}\left(k_z\frac{\delta T}{\delta z}\right) + \text{heat source} \qquad (1)$$

where T is the temperature (°C), which is a function of x, y, z and time t in seconds (s), ρ is the density of the material (kg/mm^3), k_x, k_y and k_z are the thermal conductivity in the x, y and z directions, respectively, (W/mm °C) and c is the specific heat capacity (J/kg °C). The above said physical properties are temperature dependent. The heat source is expressed as heat generation per unit volume (J/mm^3).

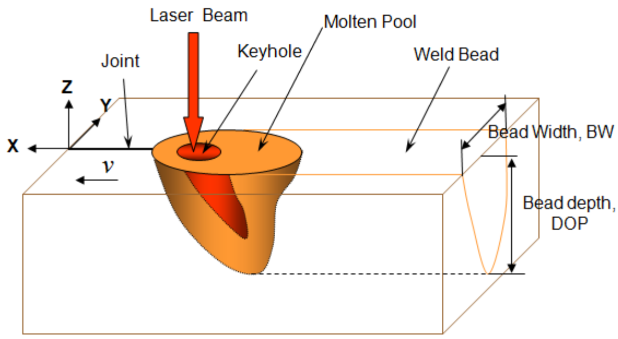

Fig.1 Schematic representation of coordinate system of laser welding process

2.1 Heat Source Modeling

In laser welding process, a part of the energy generated by the laser source is lost before absorbed by the weld specimen. The energy loss is due to the reflection from the specimen surface while rest of the energy is absorbed by the specimen. The energy loss for AISI304 stainless steel material determined experimentally by the past researchers [7] is 30.7% of the nominal power of the laser source [8]. Therefore, the absorbed energy considered for this present investigation is 69.3% of the beam power.

During simulation, consideration is given to the fact that the heat comprises a plane heat source on the top surface and a conical heat source along the thickness direction (refer Fig. 2). In that 69.3% of the beam power, the power absorbed on the surface of the specimen is 17.3% *(Q_{surf})* and the remaining 52.7% by the keyhole wall *($Q_{keyhole}$)*. Assuming that the laser beam maintains a constant Transverse

Electromagnetic mode (TEM_{00}), the Gaussian heat flux distribution $Q(x,y)$ can be expressed as:

$$Q(x,y) = \frac{3Q_{surf}}{\pi R^2} exp\left(-\frac{3(x^2+y^2)}{R^2}\right) \quad (2)$$

where Q_{surf} is heat power of the plane heat source (17.3%) and R is the heat source radius.

The radius of the heat source is calculated from the focal length of the focusing lens, which can be computed according to the relation found in

$$R = \frac{2M_0^2 \lambda F}{\pi D_0} \quad (3)$$

where M_0^2 is the value of beam quality (Nd:YAG laser with a wavelength (λ) of 1.060 µm, beam quality is 1.04), F is the focal length of the focusing lens and D_0 is the minimum diameter of the laser beam (0.3 mm). Assuming the simulation of keyhole is a cone, the Gaussian distribution of heat flux is written as

$$Q(z) = \frac{2Q_{keyhole}}{\pi r_0^2 H} e^{1-\left(r/r_0\right)^2} \left(1 - \frac{z}{H}\right) \quad (4)$$

where $Q_{keyhole}$ is the absorbed laser beam power (52%), r_0 is the initial radius (at the top of the keyhole - 0.3 mm), H is the sheet thickness, r is the current radius, i.e. the distance from the cone axis and z is the current depth [9]. The total heat input to the model is computed from the summation of surface and volume heat source models.

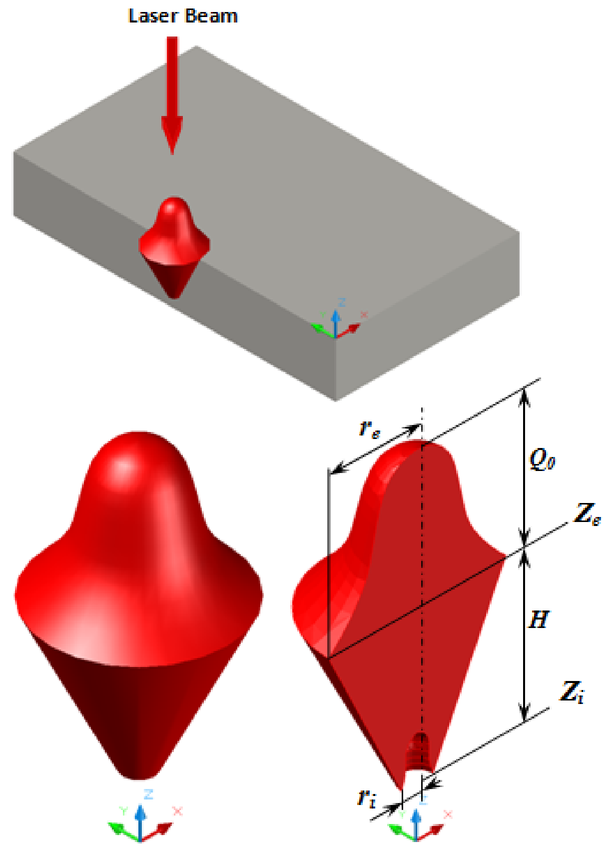

Fig. 2 Schematic of 3D Conical Heat source model

2.1.1 Material of Experimentation

The material used for this purpose is commercial AISI304 stainless steel sheet of thicknesses 1.0 and 1.6mm. The chemical composition of this material under annealed condition is presented in Table 1. Thermo-physical properties (temperature dependent) of the material are assumed to be isotropic and homogeneous and are taken according to Sabbaghzadeh et al [3]. The latent heat of fusion is 247 kJ/kg, to be released or absorbed over the range of temperature between T_S = 1400°C and T_L = 1500°C and the latent heat of vaporization is 7600 kJ/kg [5] (above 2467°C).

Table 1: Chemical composition of AISI304 stainless sheet metal vs. the weight percentage

C	Cr	Fe	Mn	Ni	P	S	Si
0.055	18.28	66.34	1.00	8.48	0.029	0.005	0.6

3 Laser Welding Parameters

A GSI Lumonics JK2000 welding system available at WRI, BHEL, Trichy is employed for the present study. The welding parameters chosen for the analysis are listed in the Table 2. The parameters are selected based on the expertise available at Welding Research Institute, BHEL, Trichy, where laser welding was successfully used for many industrial applications like welding of fins, batteries, dental clips etc.

Table 2: Laser welding parameters

Sl. No.	Beam Power (BP), watts	Welding Speed (WS), mm/min	Beam Angle (BA), deg.	Focal Length (F), mm
1	1000	500	85	120
2		600		
3	1250	700		
4		800		160
5	1500	900		
6		1000		

4 Finite Element Modeling

Three dimensional finite element model is developed for lap joint configuration to simulate the laser welding process using the commercial code SYSWELD. The models are used to predict the temperature distribution and weld geometry for the laser welding process of a thin walled structure (sheet) of AISI 304 stainless steel (SS304). The geometry and finite element mesh used in the model are given in Table 3. The whole solution domain is

ISBN: 978-1-61804-142-5

discretized into uniform 8-node hexahedron elements. The following assumptions are made while developing the finite element model.

- The workpiece initial temperature is 30°C.
- Thermal properties of the material such as conductivity, specific heat, density are temperature dependent.
- The convection and radiation loads are considered.
- There is no predefined weld bead geometry.
- In lap joint configuration, the lapped region alone is considered for the analysis purpose.

Table 3 Finite element mesh and geometry to simulate the laser welding process for lap joint configuration

<table>
<tr><td>No. of Nodes – 55927
No. of Elements – 50362</td></tr>
<tr><td>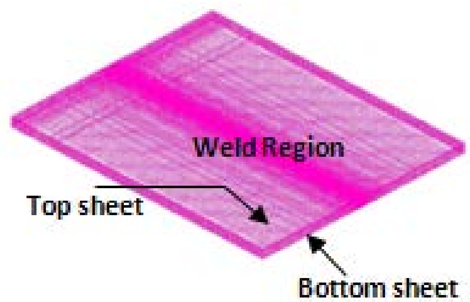
</td></tr>
<tr><td>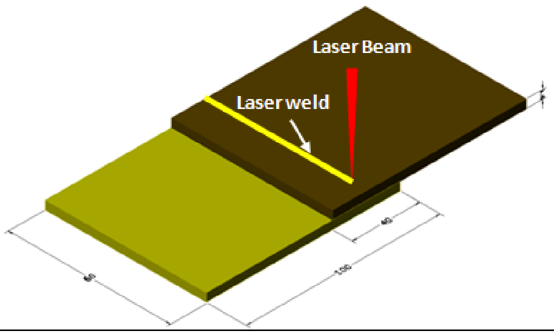
</td></tr>
</table>

4 Results and Discussions

FE simulations using SYSWELD for lap joints are run for the combinations of laser welding parameters adopted for experimental trials. Hence, the validation of computed results from FE model and general applicability of adaptive volumetric heat source is ensured. In addition, the finite element model is also validated with a set of experimentally measured lap joint weld dimensions.

Finite element simulation of lap joint welding is carried out for each welding condition listed in Table 3 to determine the weld geometry, i.e. bead width and depth of penetration taking the material properties for 1.0 mm thick AISI 304 SS sheets. Fig. 3 presents the temperature contours at four different time periods during the laser irradiation for one of the cases, where the beam power is 1250 W, welding speed is 700 mm/min and the beam angle is 85°, from which the high temperature gradients in the vicinity of the weld line close to the laser source may be clearly observed. The heat inputs generated by the moving heat source along the weld line are gradually transferred in all directions of the sheet by conduction, convection and radiation. As can be seen from the figure, the temperature around the laser source reaches around 3934°C suggesting vaporisation of material in the fusion zone. However, the temperature around the edge where the welding is started is decreased greatly to the range of 997°C. It can be seen that the laser source preheats a very small area in front of the laser source where the heat source is going to pass.

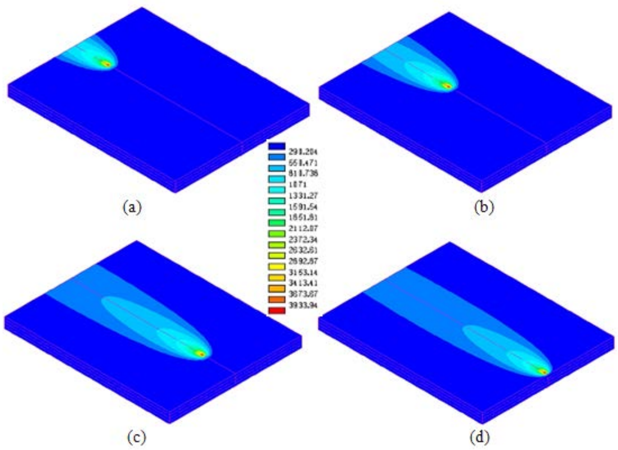

Fig. 3 Temperature distributions during the welding process at four different time periods (a) 1.28 s, (b) 2.49 s, (c) 4.50 s and (d) 5.85 s

The influence of the beam power on the bead shape with a fixed welding speed of 700 mm/min and spot diameter of 0.8 mm is shown in Fig. 4. From this result, one can infer that both the penetration depth and bead width increases as beam power increases. From the simulation result, it is observed that at higher beam power (1500 W) proper fusion of top and bottom sheets are achieved, whereas at lower beam power (1000 W) the top sheet alone is melted and there is no penetration in the bottom sheet. Further, the increase in beam power leads to an increase in the heat input, therefore, more molten metal and consequently more

ISBN: 978-1-61804-142-5

penetration depth is achieved. However, the idea is reversed in the case of weld speed effect, because the welding speed has an opposite effect to that of beam power. Fig. 5 shows the dependence of the welding penetration depth and bead width on the welding speed for a beam power of 1500 W and spot diameter of 0.8 mm. The trend of decrease in penetration depth and bead width with increase of the welding speed can be noticed. It can be explained by the fact that the amount of heat conduction transmitted to the base metal decreasing as the welding speed increases.

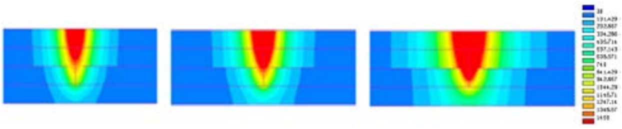

(a) (b) (c)

Fig. 4 Effect of beam power (a) 1000 W, (b) 1250 W and (c) 1500 W on weld bead geometry at constant welding speed of 700 mm/min and spot diameter of 0.8 mm

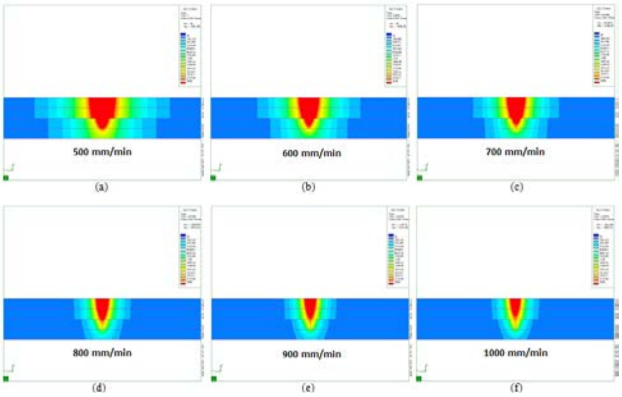

Fig. 5 Effect of welding speed on weld bead geometry at constant beam power of 1500 W and spot diameter of 0.8 mm

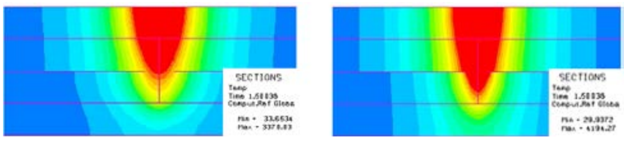

(a)

(b)

Fig. 6 Effect of Spot diameter (a) 0.8 mm and (b) 0.6 mm on weld bead geometries at constant beam power of 1500 W and welding speed of 1000 mm/min

Fig. 6 shows typical result of the effect of spot diameter on weld bead geometry for specimen thicknesses of 1.0 + 1.0 mm. It is observed that a focused beam of small diameter (0.6 mm) results in increase in the power density of the beam, resulting in better penetration depth. Once the spot diameter of the beam is increased, the laser beam becomes wider resulting in the beam energy exposed to wide area. Therefore, wide area of the base metal will melt leading to an increase in bead width. To achieve maximum penetration depth the beam power has to be maintained at higher level with minimum spot diameter of the beam, while welding speed has to be minimum.

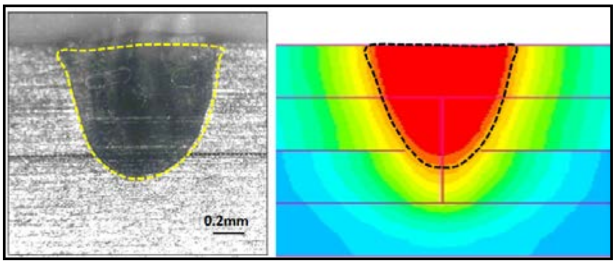

(a) (b)

Fig. 7 Comparison of calculated result with experimental one for beam power of 1250 W, welding speed of 800 mm/min and spot diameter of 0.8 mm and workpiece thickness of 1.0+1.0mm (a) Sectioned specimen and (b) Contour of calculated melting temperature

Fig. 7 shows comparison of cross section of bead profile obtained from experiment and simulation for the thickness combination of 1.0 + 1.0 mm with beam power of 1250 W and welding speed of 800 mm/min. The comparison shows that the bead width and penetration depth calculated by simulation agree well with the experimental result with an error of about 2%. Fig. 8 shows the comparison between the calculated and the corresponding measured weld pool dimensions i.e. bead width and penetration depth for all cases of the beam powers and welding speeds considered in the present work. It can be observed from Fig. 8 (a) and (b) that the bead width and penetration depth decrease linearly with the increase in the welding speed. The bead width decreases from 1.5 to 1.13 mm and decrease in the penetration depth from 2 to 1.15 mm with increasing welding speed from 500 to 1000 mm/min at a constant beam power of 1500 W, spot diameter of 0.8 mm and specimen thickness of 1.0 + 1.0 mm. Further, it is concluded from the results that the FEM simulations predict the penetration depth and bead width within a maximum error of about ±5%. A similar type of observation is also noticed for another thickness combination of 1.6 + 1.6 mm considered in this work.

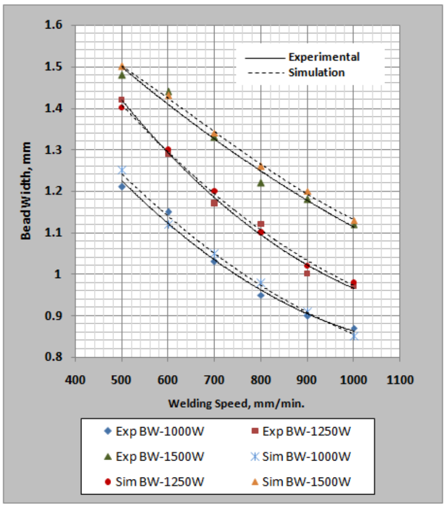

(a)

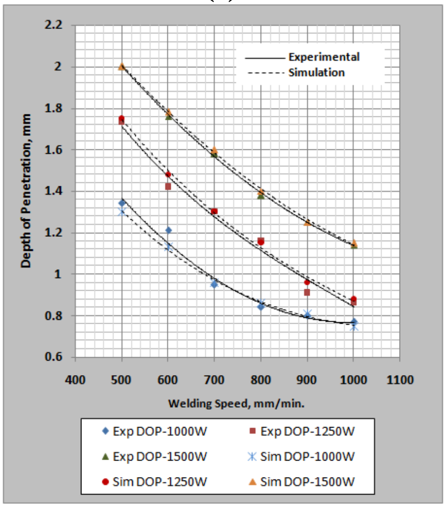

(b)

Fig. 8 Comparison of computed weld dimensions (a) Bead width and (b) Depth of penetration with corresponding measured results

5 Conclusions

This research work employs the finite element code SYSWELD to model the thermal field and bead shape for the laser welding of Lap joint configuration. Based on the research study conducted, the main conclusions can be summarized as follows:

- A moving three dimensional Gaussian heat source model has been implemented into FE thermal simulations to predict welding temperature distributions.
- The results demonstrate that the beam power, welding speed, beam incident angle and beam spot diameter have important effects on the temperature distribution and thus on the weld bead profiles.
- The peak temperature values of the upper and the lower surface increase with increase of the beam power, but decrease with increase of the welding speed. The temperature difference in the thickness direction increases with increase of the beam power and decreases with increase of the welding speed.
- Further, it can be seen that the spot diameter of the laser beam plays a predominant role in achieving a higher penetration depth with minimum bead width.

References:

[1] T.L. Teng, C.P. Fung, P.H. Chang and W.C. Yang, Analysis of residual stresses and distortions in T-joint fillet welds, *International Journal of Pressure Vessels and Piping, 78*, 2001, pp. 523-538.

[2] D. Rosenthal, The Theory of Moving Source of Heat and it's Application to Metal Treatment,' *Trans. ASME, 68*, 1946, pp. 849–866.

[3] J. Sabbaghzadeh, M. Azizi and M.J. Torkamany, Numerical and experimental investigation of seam welding with a pulsed laser, *Journal of Optics & Laser Technology, 40*, 2008, pp. 289-296.

[4] R. Spina, L. Tricarico, G. Basile and T. Sibillano, Thermo-mechanical modeling of laser welding of AA5083 sheets, *Journal of Materials Processing Technology, 191*, 2007, pp. 215-219.

[5] W.S. Chang and S.J. Na, Prediction of laser spot weld shape by numerical analysis and neural network, *Metallurgical and Material Transactions B, 32B*, August 2001, pp 723-731.

[6] G. Tsoukantas and G. Chryssolouris, Theoretical and experimental analysis of the remote welding process on thin, lap-joined AISI 304 sheets, International Journal of Advanced Manufacturing Technology, Vol. 35, No. 9 - 10, 2008, pp 880 – 894

[7] J. Xie and A. Kar, Laser Welding of Thin Sheet Steel with Surface Oxidation, *Welding Research Supplement, 78*, 1999, pp. 343s – 348s.

[8] C. Carmignani, R. Mares and G. Toselli, Transient finite element analysis of deep penetration laser welding process in a singlepass butt-welded thick steel plate, *Journal of Computational Methods in Applied Mechanics and Engineering*, 179, 1999, pp. 197-124.

[9] S.A. Tsirkas, P. Papanikos and Th. Kermanidis, Numerical simulation of the laser welding process in butt-joint specimens, *Journal of Materials Processing Technology, 134*, 2003, pp 59-69.